LiDAR aided Wireless Networks - LoS Detection and Prediction based on Static Maps

Nalin Jayaweera[1], Dileepa Marasinghe[1], Nandana Rajatheva[1],
Sami Hakola[2], Timo Koskela[2], Oskari Tervo[2], Juha Karjalainen[2], Esa Tiirola[2], Jari Hulkkonen[2]
[1]Centre for Wireless Communications, University of Oulu, Oulu, Finland
[2]Nokia Standards, Oulu, Finland
{nalin.jayaweera, dileepa.marasinghe, nandana.rajatheva}@oulu.fi,
{sami.hakola, timo.koskela, oskari.tervo, juha.p1.karjalainen, esa.tiirola, jari.hulkkonen}@nokia-bell-labs.com

***Abstract*—The mmWave communication up to 71 GHz is already specified in 3rd generation partnership project (3GPP) 5G New Radio (NR), and communication in sub-THz bands is being studied for 6G widely in the academia and industry. Operation with very narrow beamwidths and much higher bandwidths in contrast to Frequency Range 1 (sub-6 GHz) can cater to the high data rate requirements at the expense of extra signal processing burden to overcome the unfavourable conditions such as high attenuation and scattering in the presence of obstacles. Such severe signal power attenuation caused by an obstacle may degrade the network performance due to link failures occurring as a result of line-of-sight (LoS) to non-LoS (NLoS) transitions. These limitations raise the necessity of a sensing system to collect situational awareness data to assist the wireless communication network. This work proposes a method to improve the LoS detection and user localization accuracy using multiple light detection and ranging (LiDAR) sensors co-located in access points (APs). We also propose an approach to predict the LoS transitions based on static LiDAR maps and the proposed method detected the LoS transition 400ms before its occurrence.**

***Index Terms*—LiDAR, 5G, 6G, vision aided communications, mmWave, THz, LoS, NLoS.**

I. Introduction

The emergence of bandwidth-hungry applications like virtual reality, wearable technology, vehicular communication created the platform for the beam-based wireless communication networks operating at Frequency Range 2 (24.25 GHz to 71 GHz) or sub-THz to be a prominent candidate for future wireless networks. The blessing of extremely wide bandwidths of such frequencies helps to achieve data rates up to 20 Gbps [1]. Their short wavelengths significantly reduce the form factor of the hardware, while narrow beams allow exploiting the spatial diversity. Such benefits come at the expense of limited cell coverage due to high signal attenuation. Another main challenge for higher frequency communications is its sensitivity to the presence of obstacles that cause signal blockage between the transmitter (Tx) and the receiver (Rx). In the presence of an obstacle, Tx-Rx beam pair link performance significantly deteriorates, and there is a high possibility of a link failure due to its high carrier frequency and lower diffraction properties . If a link fails due to a blockage, the wireless network needs to find an unblocked path or scan for a new beam pair link that corrects the beam misalignment . Thus, the beam recovery process causes extra latency to recover the beam pair and degrade the signal quality and reliability. If the communication system has knowledge about the obstacles in the proximity of a serving user, it can avoid the potential link failures before they occur by performing predictive operations. In addition, the accuracy of the user location information and obstacle detection become paramount. These facts justify the necessity of a complementary sensing system to assist the traditional wireless networks to expand their capabilities to meet the rising stringent requirements of the future wireless networks.

Ongoing discussions and proposals in 3GPP, towards NR Release-19 (5G-Advanced) reveal the interest in cooperative communication and sensing to enhance communication-related operations in future wireless communication networks. The related discussions have started in the SA1 working group responsible for Service and System Aspects [2]. Sensing-assisted communication is a key area where radio frequency (RF) or non-RF sensor data is used to optimize communication-related operations. The RF sensing has proven its capability on user detection up to several tens of centimetres, even though the ability to detect surrounding obstacles is uncertain . Moreover, it consumes RF resources and introduces a burden on RF interference mitigation which increase the implementation complexity of the APs. On the contrary, non-RF sensors such as cameras and LiDARs can provide accurate information about the environment to the communication network without interrupting network operations. The camera technology introduces privacy concerns which restricts its installation everywhere . Improved sensing accuracy, higher resolution and the longer range give edge to the LiDAR sensor to be the most promising candidate to enable the vision for future wireless networks. LiDAR uses a laser, in a range and energy that is not considered harmful to eyes, to measure the distance to an object based on the time-of-flight. Such measurements provide a detailed 3-dimensional (3D) point cloud as output which can be introduced as a digital twin of the physical environment. Furthermore, the network-based sensing approach provides the global perception of the environment to extract required information for the wireless networks, such as

the user and blockage positions, compared to the user-based sensing. Utilizing the existing sensors in the infrastructure or a separate sensor network will impose limitations on the scalability of network-based sensing. Thus, the inclusion of the sensor as a part of the AP simplifies the network and assist in sharing the sensor data within the communication network.

Motivated by the emergence of sensing-assisted communication and the limitations faced by higher frequency communications, this work proposes a method to improve the LoS detection accuracy using multiple LiDARs co-located with APs. We further solve the static blockage prediction problem by utilizing the aforementioned LoS-detection method and using the static LiDAR maps captured by the LiDARs.

II. Related work

In our previous works, we have discussed the effectiveness of utilizing infrastructure based elevated LiDARs to optimize the performance of wireless networks while reducing the burden on radio links [3]. Moreover, the fusion of multiple LiDAR point clouds from different angles yields better accuracy on measurements compared to a single LiDAR [4]. In a recent work, we proposed a method to predict human blockages using infrastructure-mounted LiDARs in indoor scenarios [5]. Human detection using LiDAR data has been a highly discussed research topic in the last decade [6]. A deep learning-based LoS detection and beam selection method has been proposed in [7]. This work considers a single LiDAR located at the base station, and they obtained an accuracy higher than 70% for LoS detection. Apart from using LiDAR data, a novel deep learning architecture for link blockage prediction using beamforming vectors and RGB images has been proposed in [8]. Furthermore, authors in [9] discuss about the importance of infrastructure-mounted sensors to minimize overhead of mmWave array configuration and future research directions.

III. Proposed Solution

In this work, we consider an indoor hotspot scenario where I APs serve J users. Each AP is equipped with a LiDAR sensor to collect situational awareness data without utilizing radio resources. A back-haul link connects the set of LiDAR-integrated-APs (LiAPs) to a central location (CL) which is responsible to perform the global tasks as shown in Fig. 1.

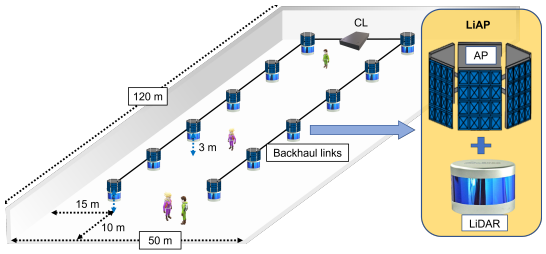

Fig. 1. The LiAP system

The installation of a LiDAR at the AP transforms the LoS detection problem in wireless networks to a human detection problem in the LiDAR point cloud. In other words, if the ith LiAP detects a human, a LoS link exists between ith LiAP and the corresponding user. We assume that any considered human in the indoor premises is an active user from the wireless network perspective, and LiAPs are placed such that a user is ensured the LoS state with at least with one LiAP. If ith LiAP fails to detect a user and other LiAPs report a user, a LoS link does not exist between ith LiAP and the corresponding user. Even though there are sophisticated LiDAR point-cloud based human detection algorithms with higher accuracy, there is still a possibility of misdetection due to body features or postures of the user. The voxelization of high-resolution point clouds to down-sample the resolution, and the imperfect denoising capability of the algorithms contribute to this misdetection significantly. Similarly, the same reasons can increase the probability of false detections. Therefore, we propose a common agreement based user detection method (CAM) to improve the user detection accuracy of the LiAP network by using the information obtained from the neighbouring LiAPs. This approach significantly improves the LoS detection accuracy.

A. LoS detection with CAM

In an environment with multiple LiAPs, a user could be visible to many LiAPs. In the initial user detection phase, each LiAP performs the user detection using its voxelized LiDAR point cloud. Let's assume the probability of detecting jth user from ith LiAP using its voxelized point cloud is $p_{i,j}$. In case of a user detection, the particular LiAP votes for a detection and reports the location of the detected user to the CL. The CAM running in CL utilizes multiple perceptions to improve $p_{i,j}$ using voting mechanism. The method can be described as follows:

- Based on the information received from LiAPs, CL defines $\mathbf{a} \in (0,1)^{I \times J}$, where $a_{i,j}$ is a binary parameter for detection of the jth user by the ith LiAP where it is 1 in case of detection and 0 otherwise. The location vector $L \in \mathbb{R}^{J \times 2}$ contains xy coordinates[1] of the detected users in the same order as in $\mathbf{a}$. Then the CL transfers L back to LiAPs.
- The ith LiAP validates the received L vector with the locations obtained in the initial user detection phase. The original point cloud prior to voxelization is used for this validation process to improve the detection accuracy. For example, a simple validation can be performed by analysing the point density around the locations found in L by fitting a bounding box. If the LiAP fails to detects a user on the jth location L_j, it updates L_j to 0. Otherwise the value in L_j is kept unchanged. The updated L is sent back to the CL.
- The CL updates $\mathbf{a}$ with newly received L vectors and the probability of false detections is minimized by imposing a voting threshold (δ). Let the number of votes received for the user $\bar{j}$ be $v_{\bar{j}} = \sum_{i=1}^{I} a_{i,\bar{j}}$ and if $v_{\bar{j}} < \delta$, the CL sets $a_{i,\bar{j}} = 0, \forall i$ to remove the false user detection $\bar{j}$. Note that

[1] Average location has been considered if many LiAPs report the same user.

the δ should be a small value compared to the number of LiAPs. Otherwise, this thresholding results in classifying a correct user detection as a false detection, due to the less number of votes from LiAPs. Hence, δ should be determined according to I. Furthermore, the dimension of $\mathbf{a}$ can be higher than J due to false detections in the initial user detection phase. Finally, the CL informs the updated $\mathbf{a}$ to LiAPs.

The solution obtained from CAM which is the updated $\mathbf{a}$ is the LoS mapping between LiAPs and active users. If $a_{i,j} = 1$, there exists an LoS link between ith LiAP and jth user, 0 otherwise. This approach can be extended to predict the LoS states or predict the variation of $\mathbf{a}$ which happens due to user mobility.

B. LoS prediction

By having the information on obstacles that can cause a link failure in future, proactive measures can be taken to improve the performance of the communication network rather than waiting for a link failure to take an action. Hence, this section proposes a static LiDAR map based novel LoS prediction method to recognize possible LoS transitions (LoS to NLoS or NLoS to LoS) which may occur due to static obstacles in the environment. In the previous work, we considered the moving human blockages [5]. Thus, now we focus only on the LoS transitions occurring due to static blockages present in the environment. We preform the LoS prediction with a two-step procedure. First, we identify potential boundaries which can cause a Los transition (Transition boundaries) and then the identifies boundaries are utilized for LoS transition prediction.

1) Transition boundary extraction: A 3D point cloud contains the set of coordinates where LiDAR's light rays met the reflection surfaces. Any obstacle such as walls, tables, chairs,.etc., which has a good reflectivity, can be sensed by LiDARs. Moreover, the LoS prediction followed by the obstacle detection, using a point cloud is an exhaustive process. Hence, we consider a LiDAR point cloud obtained by a LiAP in the absence of moving entities as a LoS map of the corresponding LiAP. The complexity of the LoS map can be reduced by projecting the point cloud to its ground plane while preserving the vital information in the LoS map. Even in the 2D LoS map, a tall object can be distinguished since it shows a higher point density along the boundaries of the obstacle and creates a hull which is the NLoS region of the LoS map as shown in Fig. 2a. Thus, LoS maps are composed of LoS zones and NLoS zones while users switch the link status between LoS and NLoS by crossing these transition boundaries.

Any NLoS region can be modelled as a polygon which is represented by a set of vertices, and the sub-set of sides at which a user change its LoS state is considered as the set of transition boundaries corresponding to the considered NLoS region. In this approach, we identify the possible LoS transition boundaries using the 2D projection of the LoS map. Fig. 2 shows an example scenario of the process. A simple algorithm can be implemented in LiAP to explore the discontinuities of the 2D projection, and these discontinuities create the

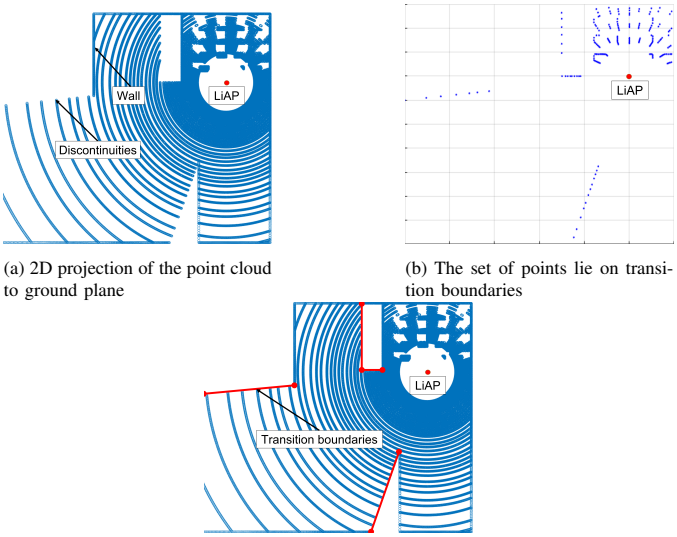

(a) 2D projection of the point cloud to ground plane

(b) The set of points lie on transition boundaries

(c) Transition boundaries

Fig. 2. The transition boundary extraction process

transition boundaries. The algorithm finds the discontinuities in the 2D projection of the static point cloud captured by LiAPs based on the orientation of k-nearest neighbouring points. For example, a highly concentrated set of points with a linear spread reflects the existence of a wall which is not a discontinuity. Hence, a wall is not a transition boundary. The transition boundaries lie on the extracted discontinued points as shown in Fig. 2b. These boundaries can be fitted with a line segment using the sequential-RANSAC algorithm [10]. These transition boundaries are marked with red lines in Fig. 2c. Note that only a few transition boundaries have been marked for clarity.

Let us define the set of LoS transition boundaries detected by ith LiAP as $\{B_{i,1}, B_{i,2}, .., B_{i,K}\}$ where kth element $B_{i,k} \in \mathbb{R}^{2\times 2}$ represents the kth LoS transition boundary in terms of two pairs of xy coordinates which represents a line-segment. The value of K will differ from one LiAP to another depending on its placement.

2) Transition boundary-based LoS prediction: Let us consider a single user located at the $L_j(t)$ location in the tth time. The CL will update $L_j(t)$ in LiAPs periodically by executing CAM. The basis of LoS prediction is formed on, the CL identifying whether the user is moving towards a transition boundary of a certain LiAP or not. Based on the transition boundaries extracted by ith LiAP and $L_j(t)$, we define the following parameters.

- The time-varying shortest distance between the current user location and kth LoS transition boundary is denoted by $d_{i,k}(t)$ is a function of $B_{i,k}$ and $L_j(t)$. The shortest distance to a line segment from a point can be calculated using simple geometry.
- The minimum distance required for a LoS transition of a user is $D^i_{min}(t)$, where $D^i_{min}(t) = \min\{d_{i,1}(t), d_{i,2}(t), .., d_{i,K}(t)\}$.

A simple approach would be to predict LoS transitions by

imposing a physical distance-based threshold (γ) on $D^i_{min}(t)$. If $D^i_{min}(t) < \gamma$, there is a high probability for a LoS transition in the near future. Otherwise, the user will potentially remain in its current LoS state for a longer duration. Fig.3 shows the aforementioned parameters and the LoS to NLoS transition zones are marked around the transition boundaries based on γ in green dashed lines. Similarly, the NLoS to LoS transition zone can be defined. Hence, we use the term transition zone to encompass both ideas.

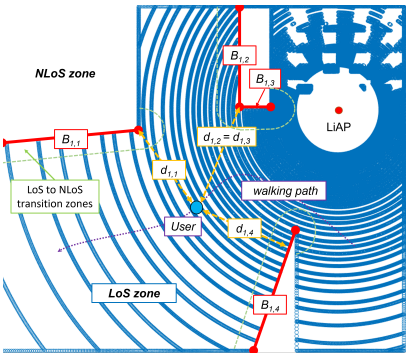

Fig. 3. Parameters

The introduction of a physical boundary to mark transition zones is not effective due to practical reasons. If the user moves parallel to a transition boundary within the transition zone still LiAP will report a possible LoS transition to the CL. Even though, these predictive measures avoid the risk of a possible link failure, such false reports reduce the performance of the wireless network. Hence, we should focus more on $D^i_{min}(t)$ when it is closer to 0, to improve the LoS prediction accuracy. To improve the sensitivity of $D^i_{min}(t)$ at its lower range, we consider the log-scale of $D^i_{min}(t)$. Moreover, we capture the converging rate of the user and the nearest transition boundary by the rate of change of $D^i_{min}(t)$ in log-scale as

$$\nabla^i(t) = \log(D^i_{min}(t)) - \log(D^i_{min}(t-1)). \quad (1)$$

Furthermore, if $\nabla^i(t) < 0$, the user is moving towards the nearest transition boundary and if user moves away from the nearest transition boundary, $\nabla^i(t) > 0$. By imposing a threshold (α) on $\nabla^i(t)$, ith LiAP reports a probable LoS transition to the CL, if $\nabla^i(t) < \alpha$. Note that the CL already has the updated LoS mapping of time-varying $\mathbf{a}(t)$. Hence, the CL is aware of the current and the next state of the radio links to make a proactive decisions such as triggering a handover to another LiAP where $D^{\bar{i}}_{min}(t)$ is high.

IV. Results and Discussion

In this work, we use the Blensor 3D animation platform to simulate and evaluate the proposed methods. The Blensor is an open-source 3D rendering tool that can simulate depth sensors such as LiDARs [11]. We consider a layout of an open office proposed by 3GPP [12] as shown in Fig. 1. Each LiAP is equipped with a rotating LiDAR: Velodyne HDL-32E LiDAR sensor, and it is placed 3 m above the ground plane. The LiDAR is set to have a scanning frequency of 10 Hz which corresponds to a 100 ms sampling period. The standard deviation of the LiDAR noise is 0.08 dB. We utilize a simple human detection algorithm based on the iterative point cloud clustering method which serves as the foundation to evaluate the proposed CAM and LoS prediction methods [13].

A. LoS detection with CAM

To evaluate the proposed CAM, we modify the floor by adding a chair, tables and walls. A set of static users with different properties are placed on the floor area as depicted in Fig. 4. We simulate six LiAPs for this evaluation. Before evaluating CAM, we present the performance of the implemented human detection algorithm as a benchmark.

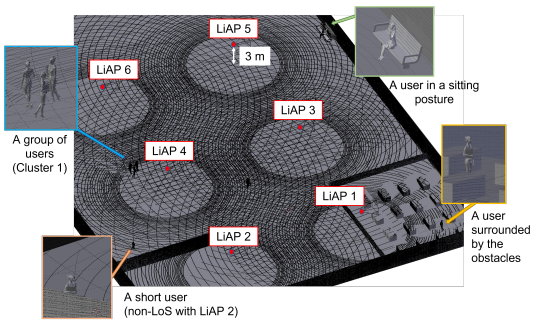

Fig. 4. An open office with 6 LiDARs collocated with APs

The users have different postures and body sizes. Furthermore, three users form a cluster (with 1 m user separation), and one user is placed near the obstacles. In the setup, the user 3 is not visible to LiAP 2, but all the other users are visible to the remaining LiAPs. In the simulations, each LiAP performs the initial user detection independently and Table I summarizes the observed results for each user after the initial detection phase and the corresponding maximum localization errors from the reported locations.

Table I: Initial user detections

j	Remarks	i=1	i=2	i=3	i=4	i=5	i=6	Maximum localization error
1	Surrounded by LiAPs	1	1	1	1	1	1	0.13 m
2	Surrounded by obstacles	1	1	1	0	0	0	0.14 m
3	Short (120 cm) & non LoS	1	0	1	1	0	1	0.15 m
4	In cluster 1	0	0	0	1	1	1	0.10 m
5	In cluster 1	0	1	1	1	1	1	1.0 m
6	In cluster 1	1	1	1	1	1	1	0.13 m
7	Sitting	0	0	0	1	0	0	0.12 m

Each detected user is assigned a unique identification by the CL. The remarks column describes the special property of the corresponding user. The localization error is the distance between exact centroid of the user and the detected centroid of the user. Maximum localization error is taken over the reported locations from the set of LiAPs for each user. The user 1 is an isolated user surrounded by LiAPs, and all LiAPs detect the user with a maximum localization error of 13 cm. The users in a cluster can be detected separately based on the distance between LiAPs and the user cluster (LiAP 4, 5 and 6 are very close to cluster 1). The posture of the user has a significant

effect on the detection. If the user stands near an obstacle or sit, the probability of misdetection is high due to the complexity of the cluster. The height of the user is not critical, yet detectable height reduces as the number of surrounding obstacles and their height increase. From the results obtained by the initial detection algorithm, we observe a maximum user localization error of 1 m when the user is in a cluster and a misdetection probability of 0.31.

Now we execute the CAM in CL on top of the initial user detection algorithm to evaluate its performance and set $\delta = 2$. Table II shows the final results obtained by the CL and the localization error of the averaged user location obtained with the CAM. The LiAP 2 fails to detect the user 3 as expected, and the visibility of the remaining users except the user 7 was confirmed by the proposed CAM. The reason for misdetection of user 7 who is in a sitting posture is the elimination due to the lack of sufficient votes from other LiAPs. Clearly, the CAM has a significant impact on the localization error which improves the localization error from 0.18 m to 0.13 m. This approach yields a misdetection probability of 0.14 which is a significant improvement compared to the initial user detection performance.

Table II: User detections enhanced by CAM

j	Remarks	i=1	i=2	i=3	i=4	i=5	i=6	Localization error
1	Surrounded by LiDARs	1	1	1	1	1	1	0.05 m
2	Surrounded by obstacles	1	1	1	1	1	1	0.10 m
3	Short (120 cm) & non LoS	1	0	1	1	1	1	0.12 m
4	In cluster 1	1	1	1	1	1	1	0.03 m
5	In cluster 1	1	1	1	1	1	1	0.41 m
6	In cluster 1	1	1	1	1	1	1	0.12 m
7	Sitting	0	0	0	0	0	0	0.12 m

B. LoS prediction

To evaluate the proposed LoS prediction method, we modify the office floor layout by adding more walls. It increases the probability of LoS transitions as a result of user mobility. Furthermore, we created a 2D map of the corresponding 3D environment and generated a path for a single user moving inside the area . For the simulations, we captured the user locations over 280 seconds[2], which corresponds to 2800 LiAP scans. For this setup, we created a dataset by activating LiAP 1, LiAP 2 and LiAP 5. Hence, the dataset is composed of 8400 LiDAR scans in total. We observed 24 LoS transitions made by the user with all 3 LiAPs activated in the dataset. We present the results of the proposed LoS prediction method in Fig. 5. The variation of $D^i_{min}(t)$ for three LiAPs ($i = 1, 2, 5$) is shown in Fig. 5a. It can be observed that the linear scale for $D^i_{min}(t)$ is inefficient as the transitions take place when $D^i_{min}(t)$ is very small. The variations of $D^i_{min}(t)$ in log-scale shows its sensitivity for lower values of $D^i_{min}(t)$ and possible LoS transitions with vertical asymptotes as depicted in Fig. 5b. Furthermore, it shows the variation of $\nabla^i(t)$ for LiAP 1 compared to $\log(D^1_{min}(t))$.

By setting the $\alpha = -0.2$, the approach predicted all the transitions that occured in the dataset. The distribution of the time taken for the actual transition after the prediction is shown in Fig.6. When we set $\alpha = -0.2$ to predict the transition, actual transition happened after 4 frames on average. Hence, the system has predicted the transitions 400 ms (on average) before the actual transition since the algorithm execution frequency is 10 Hz synchronous with the sensor rate. If we increase α, we can predict the transition a few more frames ahead at the expense of increased false transition predictions.

C. Discussion

The integration of a LiDAR sensor to an AP introduces many added advantages for the wireless network rather than utilizing the existing sensor devices in the infrastructure. Mainly, the existing infrastructure mounted sensors require customized configurations, an additional processing stage and a separate backhaul connection to deliver the intended information for the wireless network. Even though it is a cost-effective solution, it has scalability limitations, and coverage will be questionable. Nevertheless, AP equipped with a LiDAR as a single module can solve these limitations with cooperation among both entities. In contrast to a traditional AP, LiAP requires more capacity to process LiDAR point clouds locally. Alternatively, a centralized approach facilitates efficient point cloud processing at the CL which has more resources. Furthermore, fusion of the point clouds at the CL, yields a better object detection accuracy. Such an approach reduces the processing requirement at the LiAP. However, it increases the backhaul capacity requirement. Furthermore, the cost overhead of the LiAP will depend on the integrated LiDAR sensor while the power requirement is higher compared to a traditional AP.

The proposed LoS prediction method needs careful placement of the LiAPs such that the network completely covers the floor area. Furthermore, the infrequent LoS map updates should be triggered periodically or once a significant change in the environment occur. The circular void space (Fig. 3) below the rotating LiDAR sensor which is a blind spot resulting from its elevated placement can be considered as a highly probable LoS area for the LiAP. Moreover, here we discard the elevation of the UE when characterizing the transition boundaries to ensure the risk-free prediction. The LiAP and the proposed methods have the potential to address many challenges faced by wireless networks such as initial access and reduction of beam management overheads.

V. Conclusion

In this paper, we introduced APs co-located with a LiDAR sensors to solve the LoS detection and prediction problem in a mmWave communication system with static obstacles. We improve the LoS detection accuracy using a coordinated voting approach which resulted in a reduction of misdetection probability from 31% to 14% while improving the localization error by 5 cm. Furthermore, we address the LoS prediction

[2]For this evaluation, we consider a path which is not closer to the obstacles to guarantee 100% user detection accuracy and a minimum localization error (Table I).

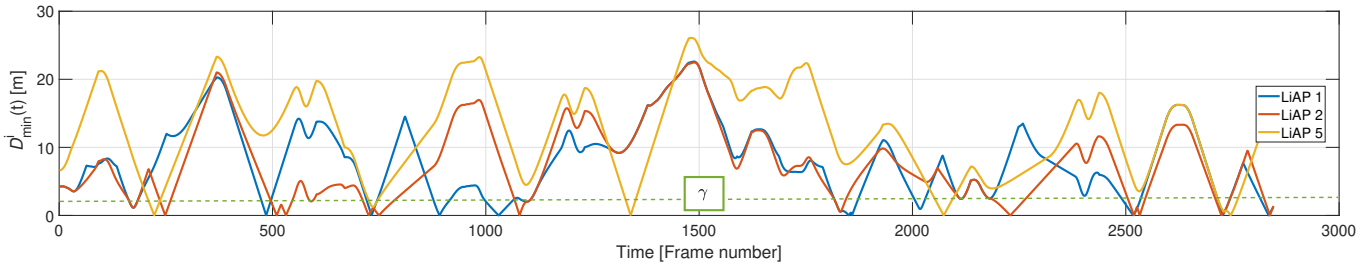

(a) Variation of $D^i_{\min}(t)$

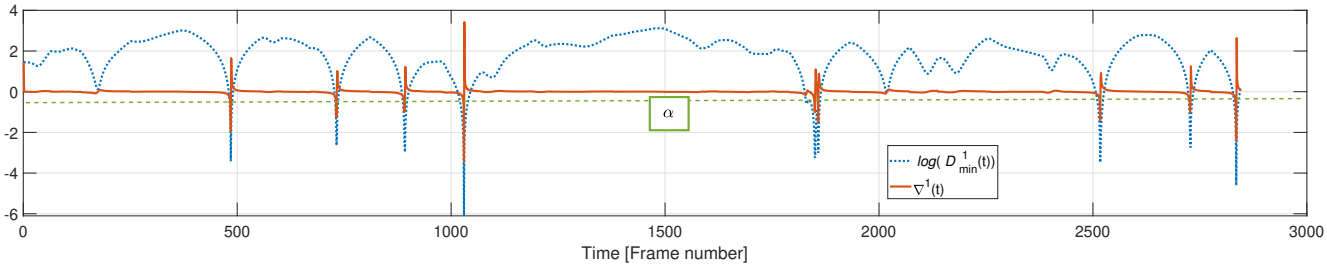

(b) Variation of $\log(D^1_{\min}(t))\nabla^1(t)$

Fig. 5. LoS prediction process

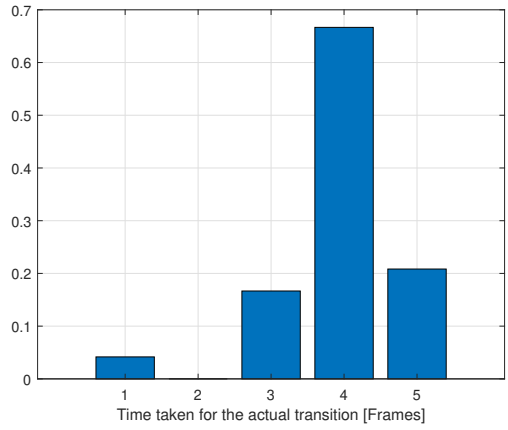

Fig. 6. Distribution of time taken for the actual transition after the prediction ($\alpha = -0.2$).

problem using a static LiDAR map. The method treated the static LiDAR map as the LoS map and extracted the probable LoS transition boundaries. The proposed LoS prediction method predicted the LoS transitions 400 ms (on average) before their occurrence, which is sufficient for the wireless communication network to take proactive measures before a possible link failure.

REFERENCES

[1] X. Wang, L. Kong, F. Kong, F. Qiu, M. Xia, S. Arnon, and G. Chen, "Millimeter Wave Communication: A Comprehensive Survey," *IEEE Communications Surveys Tutorials*, vol. 20, no. 3, pp. 1616–1653, 2018.

[2] 3GPP, "Study on Integrated Sensing and Communication," 3rd Generation Partnership Project (3GPP), New SID, 02 2022. [Online]. Available: https://www.3gpp.org/ftp/tsg_sa/WG1_Serv/TSGS1_96e_EM_Nov2021/Docs/S1-214056.zip

[3] N. Jayaweera, N. Rajatheva, and M. Latva-aho, "Autonomous driving without a burden: View from outside with elevated lidar," in *2019 IEEE 89th Vehicular Technology Conference (VTC2019-Spring)*, 2019, pp. 1–7.

[4] M. Padmal, D. Marasinghe, V. Isuru, N. Jayaweera, S. Ali, and N. Rajatheva, "Elevated lidar based sensing for 6g – 3d maps with cm level accuracy," 2021.

[5] D. Marasinghe, N. Rajatheva, and M. Latva-aho, "LiDAR Aided Human Blockage Prediction for 6G," in *2021 IEEE Globecom Workshops (GC Wkshps)*, 2021, pp. 1–6.

[6] K. Koide, J. Miura, and E. Menegatti, "A portable three-dimensional LIDAR-based system for long-term and wide-area people behavior measurement," *International Journal of Advanced Robotic Systems*, vol. 16, no. 2, p. 1729881419841532, 2019. [Online]. Available: https://doi.org/10.1177/1729881419841532

[7] M. Dias, A. Klautau, N. González-Prelcic, and R. W. Heath, "Position and LIDAR-Aided mmWave Beam Selection using Deep Learning," in *2019 IEEE 20th International Workshop on Signal Processing Advances in Wireless Communications (SPAWC)*, 2019, pp. 1–5.

[8] G. Charan, M. Alrabeiah, and A. Alkhateeb, "Vision-Aided 6G Wireless Communications: Blockage Prediction and Proactive Handoff," *IEEE Transactions on Vehicular Technology*, vol. 70, no. 10, pp. 10 193–10 208, 2021.

[9] A. Ali, N. Gonzalez-Prelcic, R. W. Heath, and A. Ghosh, "Leveraging Sensing at the Infrastructure for mmWave Communication," *IEEE Communications Magazine*, vol. 58, no. 7, pp. 84–89, 2020.

[10] X. Qian and C. Ye, "NCC-RANSAC: A fast plane extraction method for 3-D range data segmentation," *IEEE transactions on cybernetics*, vol. 44, 04 2014.

[11] M. Gschwandtner, R. Kwitt, A. Uhl, and W. Pree, "Blensor: Blender sensor simulation toolbox," in *Advances in Visual Computing*, G. Bebis, R. Boyle, B. Parvin, D. Koracin, S. Wang, K. Kyungnam, B. Benes, K. Moreland, C. Borst, S. DiVerdi, C. Yi-Jen, and J. Ming, Eds. Berlin, Heidelberg: Springer Berlin Heidelberg, 2011, pp. 199–208.

[12] 3GPP, "Study on channel model for frequencies from 0.5 to 100 GHz," 3rd Generation Partnership Project (3GPP), Technical report (TR) 38.901, 05 2017, version 14.0.0. [Online]. Available: https://www.etsi.org/deliver/etsi_tr/138900_138999/138901/14.00.00_60/tr_138901v140000p.pdf

[13] K. Liu, W. Wang, and J. Wang, "Pedestrian Detection with Lidar Point Clouds Based on Single Template Matching," *Electronics*, vol. 8, no. 7, 2019. [Online]. Available: https://www.mdpi.com/2079-9292/8/7/780